Integrative and Comparative Biology, volume 51, number 6, pp. 845–855
doi:10.1093/icb/icr074

SYMPOSIUM

Coping with Variability in Small Neuronal Networks

Ronald L. Calabrese,[1,*] Brian J. Norris,[*,†] Angela Wenning[*] and Terrence M. Wright[*]

[*]Department of Biology, Emory University, 1510 Clifton Road, Atlanta, GA 30322, USA; [†]Department of Biological Sciences, 304 Science Hall 1, California State University, San Marcos, California CA 92096, USA

From the symposium "I've Got Rhythm: Neuronal Mechanisms of Central Pattern Generators" presented at the annual meeting of the Society for Integrative and Comparative Biology, January 3–7, 2011, at Salt Lake City, Utah.

[1]E-mail: ronald.calabrese@emory.edu

Synopsis Experimental and corresponding modeling studies indicate that there is a 2- to 5-fold variation of intrinsic and synaptic parameters across animals while functional output is maintained. Here, we review experiments, using the heartbeat central pattern generator (CPG) in medicinal leeches, which explore the consequences of animal-to-animal variation in synaptic strength for coordinated motor output. We focus on a set of segmental heart motor neurons that all receive inhibitory synaptic input from the same four premotor interneurons. These four premotor inputs fire in a phase progression and the motor neurons also fire in a phase progression because of differences in synaptic strength profiles of the four inputs among segments. Our work tested the hypothesis that functional output is maintained in the face of animal-to-animal variation in the absolute strength of connections because relative strengths of the four inputs onto particular motor neurons is maintained across animals. Our experiments showed that relative strength is not strictly maintained across animals even as functional output is maintained, and animal-to-animal variations in strength of particular inputs do not correlate strongly with output phase. Further experiments measured the precise temporal pattern of the premotor inputs, the segmental synaptic strength profiles of their connections onto motor neurons, and the temporal pattern (phase progression) of those motor neurons all in the same animal for a series of 12 animals. The analysis of input and output in this sample of 12 individuals suggests that the number (four) of inputs to each motor neuron and the variability of the temporal pattern of input from the CPG across individuals weaken the influence of the strength of individual inputs. Moreover, the temporal pattern of the output varies as much across individuals as that of the input. Essentially, each animal arrives at a unique solution for how the network produces functional output.

Introduction

To make complex movements, motor networks that drive motor neurons must produce precise patterns of activity. For rhythmic behaviors such as locomotory movements and breathing, autonomously active neuronal networks called central pattern generators (CPGs) participate with sensory feedback in timing and coordinating motor neuron activity (Marder and Calabrese 1996). Since such networks can be activated in isolated parts of the nervous system and produce stereotypical output that mimics that seen under behavioral conditions, these networks have been favored objects of study for those interested in how rhythmic neuronal activity arises and is coordinated into a functional pattern. In particular, invertebrate CPGs, such as the swimmeret and stomatogastric CPGs of crustacea and the heartbeat CPG of medicinal leeches, have been intensely studied because they comprise small numbers of identifiable neurons and are thus simpler to analyze in detail (Kristan et al. 2005; Marder et al. 2005; Mulloney and Hall 2007; Smarandache et al. 2009). Detailed conductance-based models of these neuronal networks have been intimately involved in this analysis.

Driven by systematic studies of variation in parameters of conductance-based neuronal models, there is now an appreciation that a very large group of different sets of parameters, each corresponding to different maximal conductances for intrinsic membrane and synaptic current, can yield very similar network activity that is functional

Advanced Access publication June 30, 2011

(Prinz et al. 2004; Prinz 2007; Gunay et al. 2008). These modeling studies, particularly those in the stomatogastric CPGs of crustacea, have galvanized experimental studies to determine the range of animal-to-animal variation in such parameters commensurate with functional output: analysis of the stomatogastric CPGs of crustacea at the electrophysiological and molecular level has led the way. There is a 2- to 5-fold variation of intrinsic and synaptic parameters across animals, yet functional output is maintained (Marder and Goaillard 2006; Marder et al. 2007). Experimental analysis, hybrid system analysis, and theoretical analysis have led to the hypothesis that correlated compensatory changes in particular parameters can at least partially explain the biological variability in parameters (Schulz et al. 2006, 2007; Olypher and Calabrese 2007; 2009; Tobin et al. 2009; Grashow et al. 2010).

Here, we review studies in which we took advantage of our detailed knowledge of the leech heartbeat CPG and our ability easily to assess the strength of inhibitory connections from the CPG onto motor neurons to ask how the firing phase of motor neurons is determined by their inhibitory inputs and to explore the consequences of animal-to-animal variation in synaptic strength for coordinated motor output (Norris et al. 2006, 2007a,b, 2011).

Background

Medicinal leeches (*Hirudo sp*) have two tubular hearts that run the length of the body and move blood through the closed circulatory system (Thompson and Stent 1976; Krahl and Zerbst-Boroffka 1983; Wenning et al. 2004a). The beating pattern (period of beat 4–10 s) is asymmetric with one heart generating high systolic pressure through a front-directed peristaltic wave (peristaltic coordination mode) along its length, and the other generating low systolic pressure through near synchronous constriction (synchronous coordination mode) along its length. The fictive motor pattern for heartbeat is correspondingly bilaterally asymmetric (Wenning et al. 2004b). Heart (HE) motor neurons, which occur as bilateral pairs in midbody segmental ganglia 3–18 (heart motor neurons HE(3)–HE(18), indexed by midbody ganglion number) (Fig. 1A) fire in a rear-to-front progression (peristaltic coordination mode) on one side, while those on the other side fire in near synchrony (synchronous coordination mode) (Wenning et al. 2004b). Side-to-side coordination is also maintained with the HE(8) motor neurons on the two sides firing in antiphase. The asymmetry is not permanent, but rather the motor neurons of the two sides change roles (patterns) every 20–40 heartbeat cycles.

The leech heartbeat CPG consists of seven identified and well-characterized bilateral pairs of heart (HN) interneurons that occur in the first seven segmental ganglia (heart interneurons HN(1)–HN(7), indexed by midbody ganglion number) (Fig. 1A). Two additional pairs of premotor interneurons (HN(15) and HN(16), termed rear premotor interneurons), which do not feedback onto the rest, have recently been identified (Wenning et al. 2008). An unidentified HN(X) pair has only been indirectly characterized (Norris et al. 2006). This review focuses on the first seven pairs of heart interneurons, which generate the timing of the beat, implement the switches in coordination mode and provide the only inputs to motor neurons in midbody segments 7–14 (Norris et al. 2007a). In this CPG core, interneurons can be subdivided into overlapping functional groups (Fig. 1B). The first four pair of interneurons generate the timing of beat: the HN(3) and HN(4) interneuron pairs that are each linked by reciprocal inhibition drive the rhythm as independent half-center oscillators. These half-center oscillators are coordinated by the HN(1) and HN(2) interneurons. The HN(3) and HN(4) interneurons also make direct inhibitory synaptic connections with ipsilateral motor neurons and are thus designated as front premotor interneurons. These interneurons feed-forward inhibition to the HN(5) switch interneurons and excitation through electrical coupling to the middle premotor interneurons (HN(6) and HN(7)). The switch interneurons feed forward bilateral inhibition to the middle premotor interneurons (Fig. 1B). Only one of the two switch interneurons is active and bursting in the heartbeat rhythm at any given time, the other is quiescent (Fig. 1C). The active switch interneuron determines the balance of inhibition and excitation to the middle premotor interneurons on the two sides.

The temporal pattern of the activity of the premotor interneurons has been described quantitatively, and like that of the motor neurons is bilaterally asymmetric with appropriate side-to-side coordination and regular side-to-side switches of peristaltic and synchronous patterns (Norris et al. 2006, 2007b). Figure 1C shows one of these switches in the activity pattern of the premotor heart interneurons. The simultaneous recording from six heart interneurons, a bilateral pairs of [HN(3)] front premotor interneurons, a bilateral pair of [HN(7)] middle premotor interneurons, and the bilateral pair of [HN(5)] switch interneurons. The record starts with the left premotor interneurons firing in a

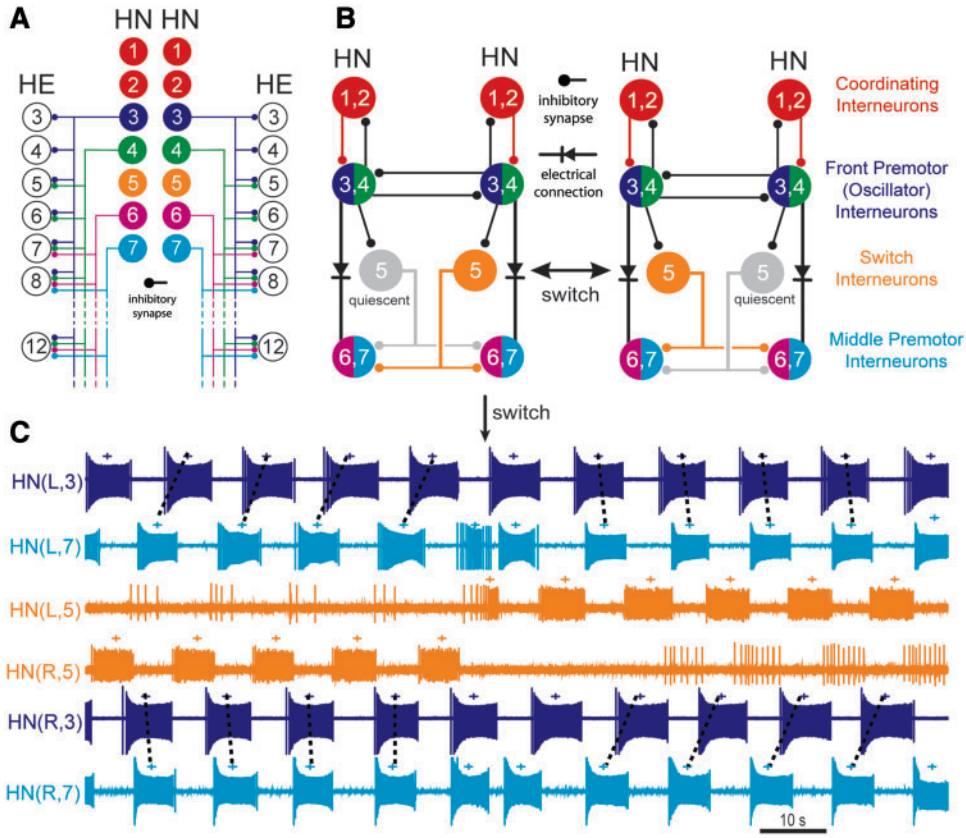

Fig. 1 The heartbeat control system of medicinal leeches: heart motor neurons and the heartbeat CPG. (**A**) Bilateral circuit diagram including all the identified heart (HN) interneurons of the core CPG showing the inhibitory connections from the heart interneurons of the leech heartbeat CPG onto heart (HE) motor neurons in the first 12 midbody segmental ganglia. The ipsilateral HN(3) and HN(4) front premotor interneurons and the ipsilateral HN(6) and HN(7) middle premotor interneurons provide input to heart motor neurons [HE(3)–HE(12)]. (**B**) Circuit diagram of the identified heart interneurons of the core CPG showing their synaptic interconnections. The two possible states of the heartbeat CPG are illustrated one with the left switch interneuron quiescent and the right switch interneuron active (corresponding to left synchronous), and the other with the left switch interneuron active and the right switch interneuron quiescent (corresponding to left peristaltic). In (A and B), large filled circles are cell bodies and associated input processes. Lines indicate cell processes and small filled circles indicate inhibitory chemical synapses. Electrical connections are indicated by a diode symbol. Heart interneurons that have similar input and output connections are lumped together for ease of presentation. Standard colors (or gray-scale equivalents) and or symbols for the heart interneurons are used in the figures [red HN(1) and HN(2), dark blue circle HN(3), dark green triangle HN(4), magenta square HN(6) and cyan diamond HN(7)]. (**C**) Simultaneous recordings of a bilateral pair of front premotor interneurons [HN(3)], a bilateral pair of middle premotor interneurons [HN(7)], and the bilateral pair of switch interneurons [HN(5)] during a switch in coordination mode from left synchronous to left peristaltic as indicated in the circuit diagrams in B. Body side indicated by R or L in the HN index.

rear-to-front progression (peristaltic coordination mode) and the switch interneuron in a quiescent state, whereas the right premotor interneurons are firing in near synchrony (synchronous coordination mode) and the right switch interneuron is in an active state; precipitously the sides switch modes reciprocally as the quiescent switch interneuron becomes active and the active switch interneuron becomes quiescent. Note the abrupt change in the activity states of the switch interneurons shifts the firing phase of the middle premotor interneurons but not of the front premotor interneurons and that the switch is complete in one cycle.

The temporal pattern of activity in the premotor interneurons is ultimately transmitted to the motor neurons to coordinate them into peristaltic and synchronous motor patterns (Fig. 2) by the pattern and strength of their inhibitory connections to the motor neurons. The pattern and strength of the inhibitory connections from the premotor interneurons to the motor neurons (segmental synaptic strength profiles) have been quantitatively described by spike-triggered averaging (Fig. 3) and is bilaterally symmetric (Norris et al. 2007a). In the region that we focus on here, motor neurons HE(8)–HE(12), all the motor neuron receive the same pattern of

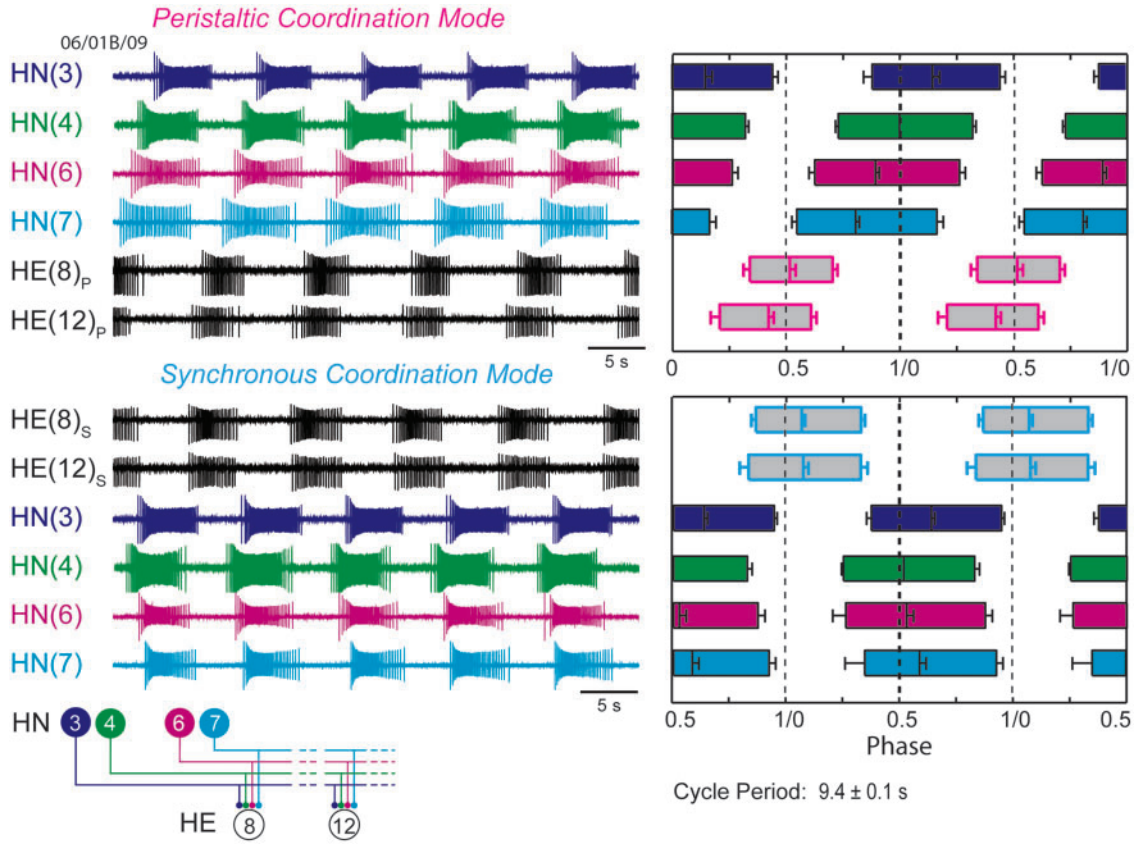

Fig. 2 The two coordination modes (peristaltic and synchronous) of the heart motor neurons and heart interneurons shown in primary recordings and as phase diagrams. Left panels: simultaneous extracellular recordings were made of ipsilateral HN(3), HN(4), HN(6), and HN(7) premotor interneurons (inputs) and HE(8) and HE (12) motor neurons (outputs) (black) in both peristaltic (*P*) and synchronous (s) coordination modes. Right panels: summary phase diagram of the premotor interneurons [standard color (or gray scale) code] and the HE(8) and HE(12) motor neurons in both the peristaltic and synchronous coordination modes. For both motor neurons and interneurons, the average duty cycle is indicated by the length of the bar; the left edge of each bar indicates the average phase of the first spike of the burst and the right edge indicates the average phase of the last spike of the burst. Average middle spike phase (referred to simply as phase throughout the text) is indicated by a vertical line within the bar. Error bars indicate standard deviations. A phase diagram of the interneurons was first constructed from measurements of activity phase relative to the ipsilateral HN(4) interneuron's middle spike for both synchronous and peristaltic coordination modes. To align these ipsilateral phase diagrams the synchronous HN(4) interneuron was assigned a phase of 0.511, as measured with respect to the peristaltic HN(4) interneuron in bilateral recordings (Norris et al. 2006). All other synchronous interneurons were then offset by the same amount as the phase of the synchronous HN(4) interneuron. These types of recordings and analyzes were used to determine the input and output temporal pattern of the HE(8) and HE (12) motor neurons in individual animals; see Fig. 6. Adapted from Norris et al. (2011).

connections; each ipsilateral front and middle premotor interneuron connects to each motor neuron (Figs 1A, 2 and 3). Therefore, any differences in the firing time of the motor neurons in the different segments (as seen, e.g. in the peristaltic mode) must result from difference in the profile of strengths of these connections. There are distinct segmental trends in these synaptic strength profiles (Fig. 4A). The synaptic strengths of the premotor interneurons are different both across segments and within a given segment, i.e. the segmental input patterns to the HE(8), HE(10), and HE(12) motor neurons are different across animals (one-way ANOVA on the data of Fig. 4A showed significant differences both between segments for each premotor interneuron [HN(3), $F=18.11$, df$=2$, $P<0.01$; HN(4), $F=7.5$, df$=2$, $P<0.01$; HN(6), $F=5.07$, df$=2$, $P=0.01$; HN(7), $F=12.19$, df$=2$, $P<0.01$] and within a segment for the four premotor interneurons [HE(8), $F=3.06$, df$=3$, $P<0.03$; HE(10), $F=20.71$, df$=3$, $P<0.01$; HE(12), $F=22.93$, df$=3$, $P<0.01$] (Norris et al. 2011). Nevertheless, there is a large animal-to-animal variation in the strength of individual inputs (Fig. 4A).

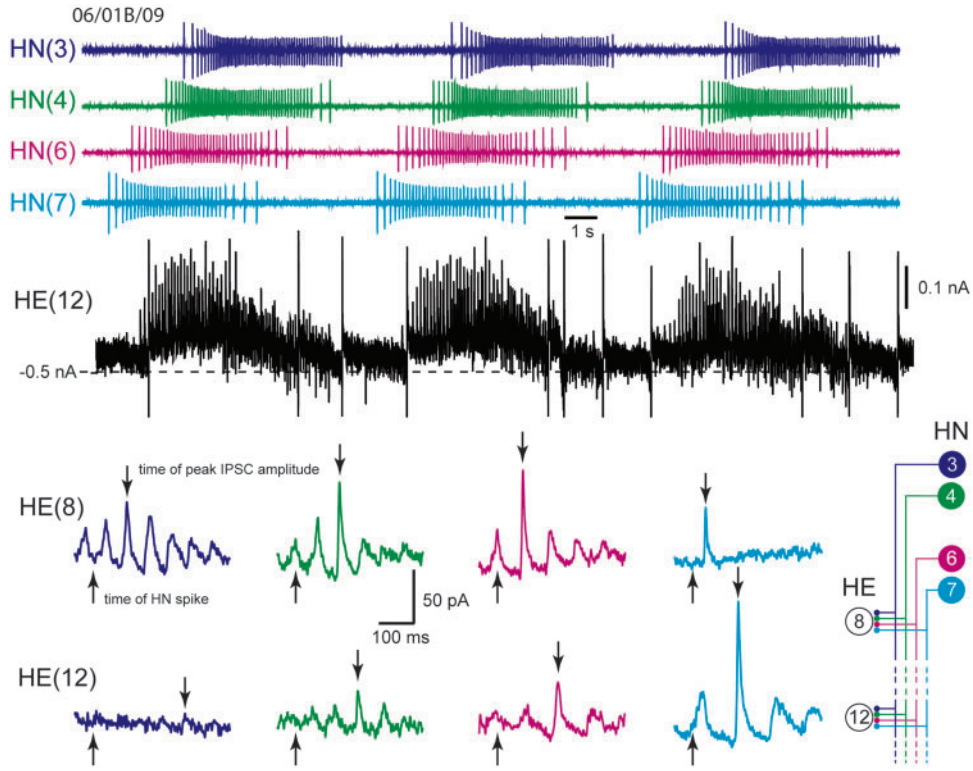

Fig. 3 The segmental synaptic strength profiles of the HE(8) and HE(12) motor neurons. In the upper panel, an HE(12) motor neuron was recorded in voltage clamp (holding potential −45 mV) simultaneously with extracellular recording from four ipsilateral premotor heart interneurons, HN(3), HN(4), HN(6), and HN(7) that provide its input. The data are from the same animal as in Fig. 2. HN spikes from ~11 bursts (including the ones illustrated) from each interneuron were used to generate the spike-triggered averages of IPSCs in the HE(12) motor neuron, and subsequently similar recordings were used to generate the spike-triggered averages of IPSCs for the HE(8) motor neuron in the same animal. Upward arrows indicate the time of the triggering HN spike and the downward arrows indicate the peak of the averaged IPSC used to measure amplitude. Spike-triggered average IPSCs, left to right arise from the HN(3)–HN(7) premotor interneurons respectively. These types of recordings were used to gather the data on synaptic strength (all currents were converted to conductances in nS using a reversal potential of −62 mV) in Fig. 4 and to characterize the HE(8) and HE(12) synaptic strength profiles in individual animals shown in Figs 5 and 6. Iconic unilateral circuit diagram (lower right) identifies the recorded neurons. Adapted from Norris et al. (2011).

The segmental synaptic strength profiles led us to a simple hypothesis for how the peristaltic phase progression is produced in the HE(8)–HE(12) motor neurons. Consider the different segmental strength profiles for the HE(8) and HE(12) motor neuron in Fig. 4A. The middle premotor interneurons are strongest in the HE(12) motor neurons and the front premotor interneurons are strongest in the HE(8) motor neuron. Since the middle premotor interneurons fire before the front premotor interneurons in the peristaltic mode, then the ipsilateral HE(12) motor neuron begins its burst earlier than the HE(8) motor neuron (Fig. 2). In the synchronous coordination mode, middle and front premotor interneurons fire together (Fig. 2), and the ipsilateral HE(12) and HE(8) motor neurons also fire together.

We have constructed a model of the entire heart motor neuron ensemble and all their inputs (Garcia et al. 2008) to test the feasibility of this hypothesis. The input to this model has two components: the temporal pattern of the premotor interneurons taken from actual recording of all four premotor interneurons in both coordination modes in a single animal like those in Fig. 2, and the segmental profiles of synaptic strength taken from data averaged across many animals. The model captures the distinct peristaltic and synchronous coordination modes of the living system but not with quantitative accuracy; e.g. the intersegmental phase difference between the HE(8) and the HE(12) motor neurons in the peristaltic coordination mode is smaller in the model than the average phase difference seen across many animals (Garcia et al. 2008). These quantitative discrepancies led us question the validity of using averaged data to determine the segmental synaptic strength profiles in the model and were our original motivation for studying animal-to-animal variation in synaptic strengths between heart interneurons and motor neurons.

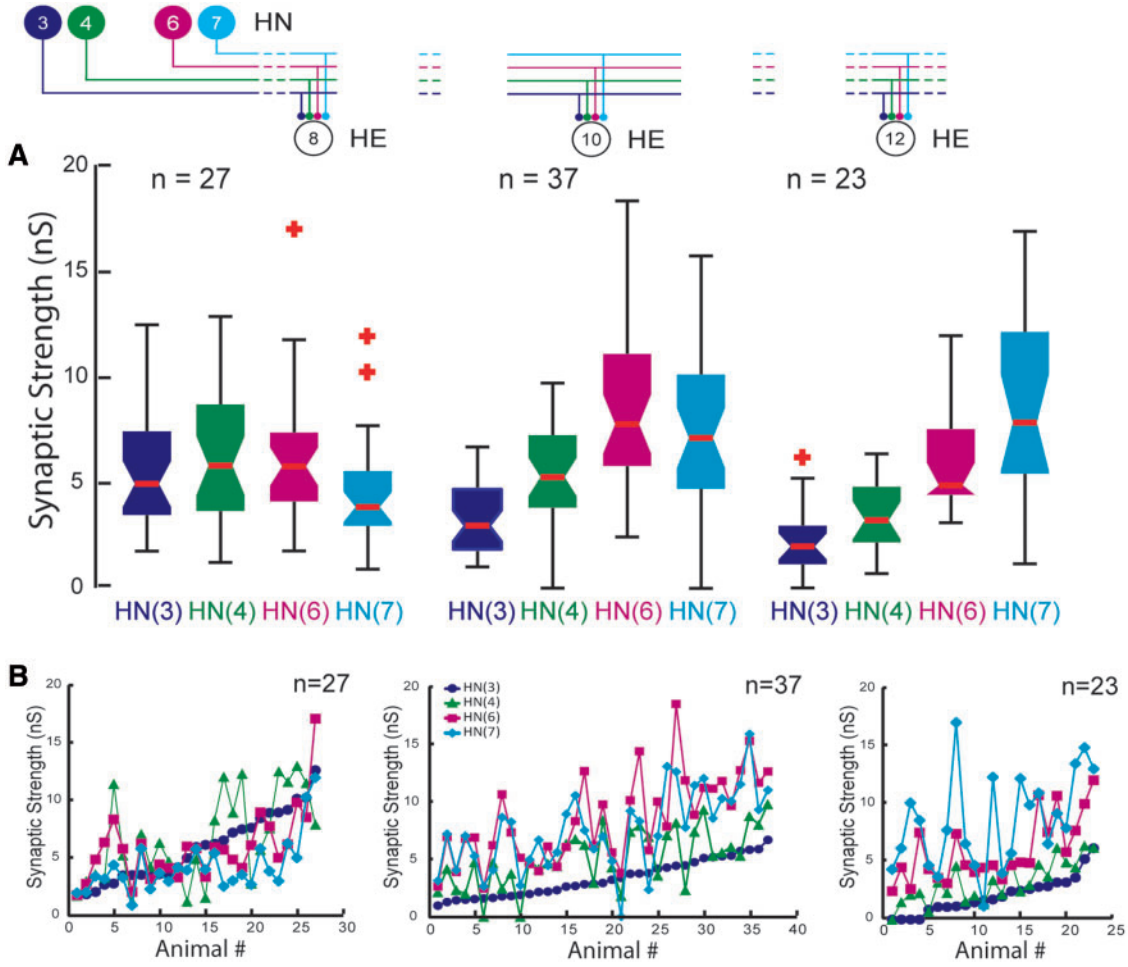

Fig. 4 Synaptic strength profiles for the inputs [from the HN(3), HN(4), HN(6), HN(7) premotor interneurons] to the HE(8), HE(10), and HE(12) motor neurons. An iconic unilateral circuit diagram (above) identifies the recorded neurons for each diagram and standard symbols are used to label each HN input in each diagram. (**A**) Whisker-Box Diagrams of synaptic strength (in nS) of inputs to the HE(8), HE(10), and HE(12) motor neurons determined from spike-trigger averages of IPSCs as in Fig. 3. Each box shows the median value at its waist and the third and first quartile at its top and base, respectively. The whisker ends indicate the lowest datum still within 1.5 × IQR (interquartile range) of the lower quartile, and the highest datum still within 1.5 × IQR of the upper quartile with outliers indicated by crosses. The strength profile across the four inputs, HN(3), HN(4), HN(6), and HN(7) interneurons, is distinctive for each motor neuron but with considerable variability in the strength of each input in each motor neuron across animals (*n*). (**B**) Viewing the animal-to-animal variation in synaptic strength illustrated in (**A**). Synaptic strength (in nS) is plotted versus animal ordered by the strength of the HN(3) input. Adapted from Norris et al. (2011).

How is animal-to-animal variability in synaptic strength accommodated?

How is the functional output of the heartbeat CPG maintained in the face of animal-to-animal variation in the strength of connections onto heart motor neurons observed across animals (Fig. 4A)? If the simple hypothesis stated above for the role of segmental synaptic strength profiles in determining motor neuron coordination in the HE(8)–HE(12) motor neurons is correct, then we reasoned that variation in the absolute strength of connections could be accommodated as long as relative strength was maintained. Therefore, we analyzed the variability in the strength of the inhibitory synapses from premotor heart interneurons onto the segmental heart motor neurons HE(8), HE(10), and HE(12) (Norris et al. 2011).

Synaptic strength profiles of the inputs to the HE(8), HE(10), and HE(12) motor neurons

Figure 4A shows that in composite that in the HE(8) motor neuron, input from the HN(4) and HN(6) interneurons predominates while the HN(3) and HN(7) inputs are at ~75% their strength, but in the HE(12) motor neuron, input from the HN(7)

interneuron greatly predominates while the HN(4) and HN(6) inputs are at ~25% its strength and the HN(3) input is very small. The HE(10) input showed an intermediate strength profile.

When the composite data of Fig. 3A are plotted individually, however, it is clear that while most individuals conform to the strength profiles observed in composite, several individuals show very different patterns (Fig. 4B) (Norris et al. 2011). For example, in the HE(12) motor neuron, input from HN(7) is usually the strongest with HN(6) sometimes having equal strength. However in one animal (animal 11) the HN(7) input is the weakest (Fig. 4B, rightmost graph); thus relative strength of the various inputs to a particular motor neuron is not maintained. It is also apparent by going left to right on the graphs of Fig. 4B that the total amount of inhibition that a motor neuron receives is not regulated; rather the sum of all the individual strengths onto a given motor neuron varies tremendously across animals. We tested whether there might be some compensatory mechanism at work such that variation in the strength of one input is compensated by an opposite variation in another input. We correlated the strength of each input against each other input for all three motor neurons and found correlations between every pair of inputs to each motor neuron that were significant, relatively strongly, and positive (Norris et al. 2011). This result indicates that such substitutive compensation does not exist.

We speculated that perhaps variations in relative strength of inputs are compensated by adjustments in the firing pattern of the premotor interneurons (temporal pattern of inputs) or reflected in the firing pattern of the motor neurons (firing phase or intersegmental phase difference). We performed experiments to measure all the relevant parameters (temporal pattern of the premotor interneurons' input, segmental strength profiles of their inputs to the motor neurons, and phase of the motor neurons all in both peristaltic and synchronous coordination modes) for the HE(8) and HE(12) motor neurons in 12 different individual leeches (Norris et al. 2011).

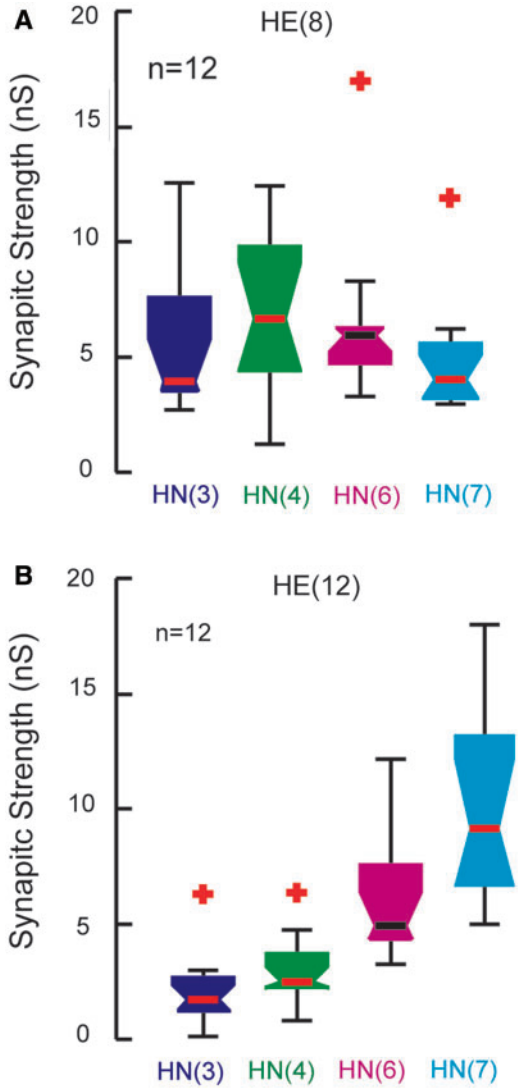

Fig. 5 Whisker-Box Diagrams of synaptic strength of inputs to the HE(8) (**A**) and HE(12) (**B**) motor neurons in 12 fully-characterized animals. Data were drawn from a series of 12 animals in which the premotor interneuronal input and output temporal patterns of the HE(8) and HE (12) motor neurons were determined as illustrated in Fig. 2 and in which the segmental synaptic strength profiles of the inputs to both motor neurons were also measured, as illustrated in Fig. 3. The strength profile across the four inputs, HN(3), HN(4), HN(6), and HN(7) interneurons is similar to that for the larger population illustrated in Fig. 4A indicating that our sample is representative. Adapted from Norris et al. (2011).

Individual animals show wide variation in temporal pattern and synaptic strength profiles of their inputs as well as temporal pattern of outputs

The process by which we analyzed each of the 12 individual animals first for temporal pattern and then for segmental synaptic strength profiles is illustrated in Figs 2 and 3. The data on strength from these experiments were combined and displayed as whisker-box diagrams (Fig. 5) to illustrate that the data from the twelve animals conforms to that from our previous experiments (Fig. 4A) (Norris et al. 2011). Figure 6 shows individualized phase diagrams with associated segmental synaptic strength profiles for a representative sample of 4 of the 12 animals analyzed (Norris et al. 2011). These maps of the temporal pattern of inputs and the temporal pattern of output, which are linked by the synaptic strength

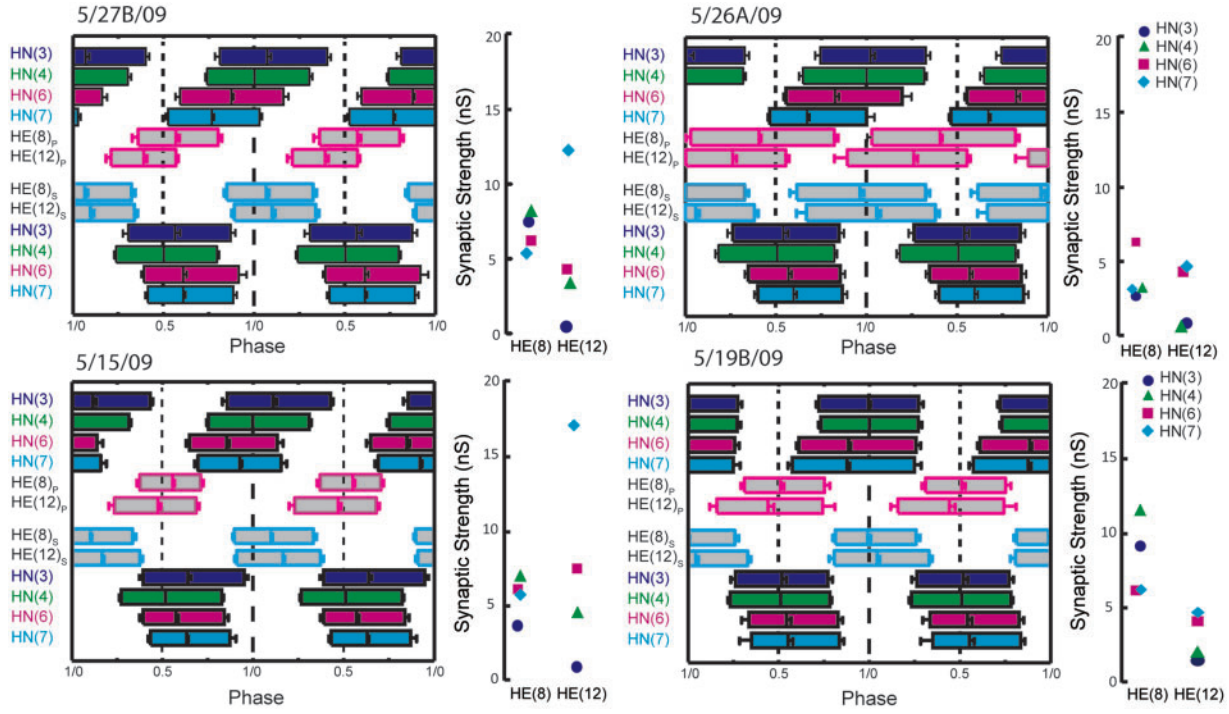

Fig. 6 Complete analysis of input and output temporal patterns and synaptic strength profiles for four different animals from our sample of 12 (summarized in Fig. 5). Temporal patterns were determined as in Fig. 2 but the two ipsilateral phase diagrams were fused into a composite for ease of presentation. The segmental synaptic strength profiles of the inputs, determined as in Fig. 3, are shown to the right of each composite phase diagram. Animals are specified by the day on which they were recorded; letters accompany the designation of day, if more than one animal was recorded on that day. Adapted from Norris et al. (2011).

profiles, show variability at all levels. The coordination modes in each are easily recognizable, but it is difficult to say how the output pattern including phase, intersegmental phase difference, and duty cycle depends on the temporal pattern or the synaptic strength profile of the input. In every case, a functional peristaltic or synchronous intersegmental pattern of motor neuron discharge is achieved; in the peristaltic mode the HE(12) motor neuron leads the HE(8) motor neuron by a minimum of 0.07 phase units (maximum of 0.18 phase units), while in the synchronous mode the HE(12) motor neuron lags the HE(8) motor neuron by a maximum of 0.09 phase units and can lead by a maximum of 0.04 phase units.

Is motor neuron phase determined by the strength and temporal pattern of each input?

We performed a correlational analysis of the phase of motor neuron discharge with synaptic strength of each input and with various strength ratios and linear combinations (Norris et al. 2011). No strong correlations between motor neuron phase and input strength were observed. Moreover, the phase difference between the HE(8) and the HE(12) motor neurons is not correlated with any of our measures of strength, in either coordination mode. The lack of observed correlations suggests that the firing of motor neurons is dependent on the entire synaptic strength profile of its inputs and not governed primarily by the strength of just one or two.

We also performed a correlational analysis of the relative phase of motor neuron discharge with phase of each input and other measures of input phase such as averages (Norris et al. 2011). We found only a few moderately strong correlations. We further performed a correlational analysis of the phase difference between the HE(8) and HE(12) motor neurons with the phase differences in their input, for the peristaltic and for synchronous modes of coordination (Norris et al. 2011). The only correlation to emerge was a weak one between the HE(8) to HE(12) phase difference and the maximum phase difference of the premotor interneurons in the synchronous mode ($R^2 = 0.34$ $P < 0.0460$). No other correlations between measures of motor neuron phases and interneuron phases were observed. The weakness

and diversity of the observed correlations suggests that the firing of motor neurons is dependent on many characteristics of the interneurons' temporal pattern and not governed primarily by just one or two.

When one considers that motor neuron phase is dependent on eight measured parameters (four HN firing phases and four HN synaptic strengths) and probably on many unmeasured parameters, like motor neuron intrinsic properties, it makes sense that our correlational analysis did not turn up many strong relationships. Implicit in this argument is the hypothesis that the phase of firing of heart motor neurons is indeed influenced by the strength of each input, but animal-to-animal variation in the other important parameters obscures these relationships. Elucidating the consequence of biological variation in any given parameter would, therefore, be greatly facilitated if all other parameters except the one in question were held constant. We used our model of the heart motor neuron ensemble (Garcia et al. 2008) to perform this feat. We varied the strength of one input at a time to each motor neuron using all 12 values for that input in our sample animals, while keeping the strength of all other inputs and the temporal pattern constant (Norris et al. 2011). We then performed similar correlational analyzes as described above for the living preparations. We found that motor neuron phase was indeed strongly correlated with the strength of each input. Apparently, variation in the phasing of premotor interneurons across animals and in the strength of other inputs obscures the correlations between motor neuron phase and premotor interneuron strength. Nevertheless, our modeling results indicate that motor neuron phase is indeed determined by the relative strength of each input when all other parameters are kept constant.

Individual animals appear to arrive at individual solutions for producing functional motor outflow from the heartbeat CPG

Given that biological variability probably obscures the contribution of individual parameters to output, how then may we express the complex relation between input and output for leech heart motor neurons? The solutions arrived at by individual animals seem currently best expressed by presenting phase diagrams with associated strength diagrams for each animals, as shown in Fig. 6.

Conclusions

Our goal originally was to determine how heart motor neurons receiving inhibitory input from a rhythmically active heartbeat CPG can produce a functional pattern of output. We quantified both the temporal pattern of input from premotor heart interneurons and the segmental strength profiles of synaptic input for these motor neurons. We used these measurements in a model of the entire heart motor neuron ensemble and were able to reproduce the characteristic peristaltic and synchronous coordination modes of the motor neurons, but not with quantitative accuracy. We hypothesized that animal-to-animal variability in synaptic strength profiles might make average data on synaptic strength inappropriate for the model [cf. Golowasch et al. (2002)]. We first tested whether relative synaptic strength within a segment was preserved across animals and found that it was not. We next concentrated on two motor neuron pairs far enough apart (midbody segments 8 and 12) to have a relatively large phase difference in the peristaltic coordination mode, yet no phase difference in the synchronous mode. Most importantly, these motor neurons receive the same complement of synaptic inputs from the same four pairs of premotor interneurons of the CPG. We then characterized a series of individual animals (12) by measuring the temporal pattern of the interneuronal input and of motor neuron output, and the segmental synaptic strength profiles of the inputs for the HE(8) and HE(12) motor neurons in each animal. After extensive correlational analysis failed to provide mechanistic insight, we came to the realization that individual animals appear to arrive at individual solutions to produce functional motor outflow from the heartbeat CPG.

Numerous theoretical and experimental studies suggest that network output can be similar despite differences in neuronal intrinsic properties and even synaptic strengths (Prinz et al. 2004; Schulz et al. 2006, 2007; Marder et al. 2007; Gunay et al. 2008; Goaillard et al. 2009; Tobin et al. 2009). Our analyzes reviewed here have now pushed this view one level deeper. The twelve animals we analyzed in detail show a wide variation in every measured parameter including input temporal pattern, segmental synaptic strength profile, and temporal pattern of motor neuron output (Fig. 6). Despite this variation, the peristaltic and synchronous coordination modes are not only perceptible in every animal at both the interneuronal and motor neuronal levels but apparently also are functionally appropriate, when compared to the animal-to-animal variation in the

blood flow patterns of intact leeches (Wenning et al. 2004a).

A corresponding study in the crustacean stomatogastric nervous system focusing on the core network of the pyloric CPG showed that the output phase of the LP motor neuron is correlated with the strengths of its two different inhibitory synaptic inputs from a pacemaker core in the network, as well as with its intrinsic membrane currents and the response of a specific membrane current to a modulator (Goaillard et al. 2009): in stark contrast to our results. There are differences in the organization of the leech heartbeat CPG and the crustacean pyloric CPG that may account for the differences in results. In the heartbeat system, the four premotor inputs are flexibly coordinated and show significant phase diversity across animals, and motor neurons do not feed back onto the premotor inputs. In the pyloric CPG, the two premotor inputs are tightly coupled electrically and act in concert as a pacemaker core. This coupling eliminates phase diversity among the inputs to the LP motor neuron. Moreover, because the LP motor neuron feeds back inhibition to the pacemaker core, input phase is partially determined by output phase (Goaillard et al. 2009). This network organization coupled with only two inputs may allow correlations to emerge. Apparently in the heartbeat system, the larger number (four) of inputs to each motor neuron, each varying in strength, and the phase diversity of the temporal pattern diminish the impact of individual inputs and confound the relationship between input strength and firing phase. On the other hand, this organization allows tremendous flexibility in arriving at functional output so that myriad individual solutions seem possible. One may then expect that in more complex systems, such as mammalian spinal CPGs, even greater flexibility and diversity in network solutions will be observed.

We were not able to measure the intrinsic properties of the heart motor neurons as was done for the LP motor neuron of the pyloric CPG (Goaillard et al. 2009), and certainly such properties must contribute to the firing phase of motor neurons. The strongest and most universal correlations we observed were between the strengths of the various inputs to each motor neuron. These correlations were all positive. This observation suggests that motor neurons vary in excitability and that all inputs must be adjusted up or down to accommodate the level of excitability. On the other hand, in a dynamic-clamp analysis of gastric motor neurons in the stomatogastric nervous system configured as half-center oscillators with reciprocal synapses and h-current, no correlations across animals of synapse strength with any of a diversity of individual excitability measures were observed (Grashow et al. 2009).

How then are we to understand how phase differences are created between heart motor neurons?

To understand how heart motor neurons in leeches are coordinated by their input into their appropriate segmental phase—both peristaltic and synchronous—we must consider the firing phase of each input, strength of each input, and the intrinsic properties of the motor neuron. Moreover, our analyzes of the twelve different animals suggest that the target values for each motor neuron output phase is itself variable across animals but somehow constrained, so that a functional peristaltic or synchronous pattern is attained. No one factor (or several factors) emerges from our analyzes as of primary importance in determining the output phase of motor neurons. Our approach now must be to use data from individual animals (Fig. 6) as both the input and the output target in conductance-based models of heart motor neurons to generate hypotheses for how they are coordinated by their inputs and what role, if any, the motor neurons' intrinsic properties play in this process.

Funding

National Institutes of Health (NS-024072 to R.L.C.).

References

Garcia PS, Wright TM, Cunningham IR, Calabrese RL. 2008. Using a model to assess the role of the spatiotemporal pattern of inhibitory input and intrasegmental electrical coupling in the intersegmental and side-to-side coordination of motor neurons by the leech heartbeat central pattern generator. J Neurophysiol 100:1354–71.

Goaillard JM, Taylor AL, Schulz DJ, Marder E. 2009. Functional consequences of animal-to-animal variation in circuit parameters. Nat Neurosci 12:1424–30.

Golowasch J, Goldman MS, Abbott LF, Marder E. 2002. Failure of averaging in the construction of a conductance-based neuron model. J Neurophysiol 87:1129–31.

Grashow R, Brookings T, Marder E. 2009. Reliable neuromodulation from circuits with variable underlying structure. Proc Natl Acad Sci USA 106:11742–6.

Grashow R, Brookings T, Marder E. 2010. Compensation for variable intrinsic neuronal excitability by circuit-synaptic interactions. J Neurosci 30:9145–56.

Gunay C, Edgerton JR, Jaeger D. 2008. Channel density distributions explain spiking variability in the globus pallidus: a combined physiology and computer simulation database approach. J Neurosci 28:7476–91.

Krahl B, Zerbst-Boroffka I. 1983. Blood pressure in the leech *Hirudo medicinalis*. J Exp Biol 107:163–8.

Kristan WB Jr, Calabrese RL, Friesen WO. 2005. Neuronal control of leech behavior. Prog Neurobiol 76:279–327.

Marder E, Bucher D, Schulz DJ, Taylor AL. 2005. Invertebrate central pattern generation moves along. Curr Biol 15:R685–99.

Marder E, Calabrese RL. 1996. Principles of rhythmic motor pattern generation. Physiol Rev 76:687–717.

Marder E, Goaillard JM. 2006. Variability, compensation and homeostasis in neuron and network function. Nat Rev Neurosci 7:563–74.

Marder E, Tobin AE, Grashow R. 2007. How tightly tuned are network parameters? Insight from computational and experimental studies in small rhythmic motor networks. Prog Brain Res 165:193–200.

Mulloney B, Hall WM. 2007. Local and intersegmental interactions of coordinating neurons and local circuits in the swimmeret system. J Neurophysiol 98:405–13.

Norris BJ, Weaver AL, Morris LG, Wenning A, Garcia PA, Calabrese RL. 2006. A central pattern generator producing alternative outputs: temporal pattern of premotor activity. J Neurophysiol 96:309–26.

Norris BJ, Weaver AL, Wenning A, Garcia PS, Calabrese RL. 2007a. A central pattern generator producing alternative outputs: pattern, strength, and dynamics of premotor synaptic input to leech heart motor neurons. J Neurophysiol 98:2992–3005.

Norris BJ, Weaver AL, Wenning A, Garcia PS, Calabrese RL. 2007b. A central pattern generator producing alternative outputs: phase relations of leech heart motor neurons with respect to premotor synaptic input. J Neurophysiol 98:2983–91.

Norris BJ, Wenning A, Wright TM, Calabrese RL. 2011. Constancy and variability in the output of a central pattern generator. J Neurosci 31:4663–74.

Olypher AV, Calabrese RL. 2007. Using constraints on neuronal activity to reveal compensatory changes in neuronal parameters. J Neurophysiol 98:3749–58.

Olypher AV, Calabrese RL. 2009. How does maintenance of network activity depend on endogenous dynamics of isolated neurons? Neural Comput 21:1665–82.

Prinz AA. 2007. Computational exploration of neuron and neural network models in neurobiology. Methods Mol Biol 401:167–79.

Prinz AA, Bucher D, Marder E. 2004. Similar network activity from disparate circuit parameters. Nat Neurosci 7:1345–52.

Schulz DJ, Goaillard JM, Marder E. 2006. Variable channel expression in identified single and electrically coupled neurons in different animals. Nat Neurosci 9:356–62.

Schulz DJ, Goaillard JM, Marder EE. 2007. Quantitative expression profiling of identified neurons reveals cell-specific constraints on highly variable levels of gene expression. Proc Natl Acad Sci USA 104:13187–91.

Smarandache C, Hall WM, Mulloney B. 2009. Coordination of rhythmic motor activity by gradients of synaptic strength in a neural circuit that couples modular neural oscillators. J Neurosci 29:9351–60.

Thompson WJ, Stent GS. 1976. Neuronal control of heartbeat in the medicinal leech. I. Generation of the vascular constriction rhythm by heart motor neurons. J Comp Physiol 111:261–79.

Tobin AE, Cruz-Bermudez ND, Marder E, Schulz DJ. 2009. Correlations in ion channel mRNA in rhythmically active neurons. PLoS One 4:e6742.

Wenning A, Cymbalyuk GS, Calabrese RL. 2004a. Heartbeat control in leeches. I. Constriction pattern and neural modulation of blood pressure in intact animals. J Neurophysiol 91:382–96.

Wenning A, Hill AA, Calabrese RL. 2004b. Heartbeat control in leeches. II. Fictive motor pattern. J Neurophysiol 91:397–409.

Wenning A, Norris BJ, Seaman RC, Calabrese RL. 2008. Two additional pairs of premotor heart interneurons in the leech heartbeat CPG: the more the merrier. Soc Neurosci, Abstracts 371.6/MM6.